IJBPAS, August, 2016, 5(8): 1810-1829

ISSN: 2277–4998

International Journal of Biology, Pharmacy and Allied Sciences (IJBPAS)

'A Bridge Between Laboratory and Reader'

www.ijbpas.com

INVESTIGATING THE RESPONSE OF NUCLEAR POWER PLANT SUBJECTED TO AIRCRAFT CRASH

REZA SABERI[*1], MAJID ALINEJAD[2], MIR OMID MAHDAVI KALAJAHI[3], KAMRAN SEPANLOO[4]

[*1]Nuclear Science and Technology Research Institute , P.O.Box 113658486, Tehran, Iran, Tel.: +98-82067284, E-mail: rsaberi@aeoi.org.ir

[2]Engineering Research Institute of Natural Hazard Shakhespajouh, Isfahan, Iran, Tel.: +98-82067261, malinejad@aeoi.org.ir

[3]Civil Engineering Department, K.N Toosi University of Technology,Tehran, Iran, Tel.: +98-9141067565, E-mail: omid_mahdavi@mail.kntu.ac.ir

[4]Nuclear Science and Technology Research Institute, P.O.Box 113658486, Tehran, Iran, Tel.: +98-82067230, E-mail: Ksepanloo@yahoo.com

***Corresponding Author: Reza Saberi; E-mail: rsaberi@aeoi.org.ir**

ABSTRACT

Structural safety of nuclear containment has been studied against the direct hit of Airbus A320, Boeing 707-320 and Phantom F4 aircrafts. The three dimensional numerical simulations has been conducted using ABAQUS/Explicit finite element code. The impact locations identified on the containment are mid height of containment, center of the cylindrical portion, junction of dome and cylinder, and over the cylindrical portion close to the foundation level. The reaction-time response curves have been used to assign loading of the aircrafts crash. The behavior of concrete was predicted using the damaged plasticity model while elasto-plastic material model was incorporated for steel reinforcements. Dynamic loading conditions were considered using Dynamic Increase Factor. The mid height of containment and center of cylindrical portion has

been found to experience highest deformation against each aircraft crash. It has also been found that compression damage in concrete is not critical at none of impact locations.

Keywords: Aircraft Crash, Dynamic Increase Factor (DIF), Concrete Damage Parameters, Nuclear Containment, Global Deformation of Containment.

1. INTRODUCTION

Since 2001, safety of nuclear buildings against a deliberate or accidental large commercial aircraft crash has attracted much attention worldwide. Nuclear containment must be constructed and operated in order to prevent the leakage of radiation into the surroundings. The direct hit of an aircraft may lead to local or global failure of nuclear containment. It is therefore an important issue to be studied.

Investigation on the response of containment structure against aircrafts crash is very complex. It is almost impossible to study its response through experiments. However, researchers in the past have made huge effort to estimate the response of nuclear containment under such attacks through analytical or numerical techniques. Riera (1968) with the assistance of crushing strength, proposed the loading time history for Boeing 707-320 aircraft against a rigid surface. Chelapati and Kennedy (1972) studied a Nuclear Power Plant (NPP) building subjected to accidental aircraft crash. It was shown global behavior of NPP is negligible. Abbas et al. (1995, 1996) found that is not always conservative to obtain the loading time history with supposition of rigid target. Riera (1980) more extended the topic through the incorporation of target flexibility and oblique incidence in the loading time history. Numerical analysis of fictitious building subjected to aircraft crash performed by Arros and Doumbalski (2007) using LS-DYNA code. The numerical model of Boeing 747 aircraft was made wherein wing load distributed over whole length. The obtained results were compared with Riera (1968) force history technique wherein the loading was applied over an area of 28 m^2. The analysis wherein the aircraft was simulated resulted in high frequency content in the building response in comparison with the analysis conducted with Riera (1968) force history technique. The studies in the literature led to the deduction that a fair estimate of response of containment can be obtained with using reaction-time response as the loading criterion. Furthermore, two different impact location were reported as the most critical

impact locations. Abbas et al. (1995, 1996) reported the junction of dome and cylinder as the most critical impact location. While Iqbal et al (2014) found that mid height of containment experienced most severe deformation against aircrafts crash.

In a collaborative project between the Nuclear Power Engineering Corporation (NUPEC) of Japan (2002) and the United States Nuclear Regulatory Commission (U.S.NRC), the seismic response of a Reinforced Concrete Containment Vessel (RCCV) was investigated. In this study, three dimensional numerical modeling of RCCV have been carried out to predict its response subjected to Phantom F4, Boeing 707-320 and Airbus A320 aircrafts. The impact locations identified on the RCCV are mid height of containment at the height of 28.6 m above the foundation level, near the junction of dome and cylinder at the height of 33.2 m, center of the cylindrical portion at the height of 18.6 m and over the cylindrical portion close to the foundation of containment at the height of 4 m, see Fig. 1. The analysis has been conducted using ABAQUS/Explicit finite element code. Symmetrical loading condition and containment geometry made it possible to simulate only half of the containment and symmetric boundary conditions were assigned.

2. Loading Time History for Aircrafts

There are studies accessible in literature wherein loading time history for aircrafts crash has been derived from characteristic of aircraft through analytical, numerical and experimental techniques (Riera, 1968; Sugano et al., 1993; Iliev et al., 2011). In almost all of these studies the loading time history has been obtained assuming the target as a flat rigid surface. Riera (1968) derived an analytical expression to determine force history for Boeing 707-320 aircraft with the assistance of the crushing strength. Siefert and Henkel (2014) obtained the curve for A320 via numerical simulations conducted by ABAQUS/Explicit code. Sugano et al. (1993) determined force response for Phantom F4 through experiment. In the present study, loading time histories for aircrafts crash has been employed from available studies in literature, see Fig. 2. The impacted area depends on the basis of specific characteristics of the each aircraft. It should be noted that impacted area is changing during the strike of aircrafts and the fuselage of the aircraft will hit a different region of containment than the wings. Since the objective of this paper is to

study the global response of RCCV against impact of aircrafts, the precision in the determination of impact region is not important. Hence, a circular contact area was considered to simplify the analysis. The average contact area calculated from Sadique et al. (2013) approach is 28.8 m^2 for 707-320.Considering the maximum diameter of fuselage for aircrafts, the average impacted area has been considered to be same (28.26 m^2) for each aircraft with diameter Ø 6 m.

This approach of determining the contact region provides a reasonably precise representation of aircraft loading as far as the global response of the containment is concerned. However, it is crucial to determine the accurate impact region when the purpose of investigation is to study local damage of containment caused by different parts of aircrafts. The loading time history was transformed to pressure and assigned to impact locations.

3. Geometric and FE Modeling of RCCV

A three dimensional modelling of the RCCV was made using preprocessing module of the ABAQUS/Explicit finite element code. The dimension of containment building was considered identical to that of the RCCV investigated by U.S.NRC and NUPEC (2002). It should be noticed that the containment was modeled unified with uniform thickness of 1.2 m. concrete cover was assumed to be 100 mm. The containment was doubly reinforced as detailed in Fig. 1.

The BWR Mark III type nuclear containment simulated by Iqbal et al. (2012) with solid elements and took about 47 Central Processor Unit hours on Workstation. In the present study, considering the ratio of thickness to the dimension of containment, RCCV was simulated as shell element. This method of simulation significantly decreased the analysis runtime. Reinforcement modeled as rebar layer option available in ABAQUS/CAE. The containment structure was meshed with S4R (Shell element reduced integration four node) elements.

In order to validate numerical simulation of RCCV, modal analysis was also carried out and Modal Frequencies were compared with those reported by (NUPEC) and (U.S.NRC)(2002) [10]. The Modal Frequencies were almost the same which confirmed simulation technique.

In order to get precise results within optimum computational time, the mesh in the contact area of Ø 6 m was highly refined as compared to the outer region. The element size in contact region was fixed as

120 mm ×120 mm with unity aspect ratio. In the outer region away from strike area however, the size of element was increased to 700 mm ×700 mm. The detail of meshing is described in Fig. 3. In order to study the mesh convergence, the size of concrete element changed from 120 mm×120 mm to 100 mm ×100 mm at the impact location "C" subjected to 707-320 (Fig. 3(c)). The maximum displacement in the contact region was found to be 0.0458 m and 0.04584 m for 120 mm×120 mm and 100 mm ×100 mm respectively.

4. Material Behaviors at High Strain Rate

Impact loads typically produce high strain rates in the range of 10^0-$10^2 s^{-1}$, while ordinary static strain rates is in range of 10^{-6}-$10^{-5} s^{-1}$. This high straining rate due to dynamic loading condition would alter the mechanical properties of materials.

5. Dynamic Behavior of Concrete under High Strain Rates

The mechanical properties of concrete can be totally different in the various dynamic loading condition. Under dynamic conditions, the stresses that are resisted for a certain period of time may gain values that are considerably higher than the static compressive strength. This enhancement in compressive strength has been proven to be because of inertia or viscosity effects of concrete. Lu and Xu (2004) reported that the enhancement in the dynamic tensile strength of concrete is more significant as compared to the dynamic compressive strength. Dynamic Increase Factor (DIF) is proposed in the CEB-FIP (1990) code for the enhancement in peak compressive stress (*f'c*) for strain rate increase of concrete as follows:

$$DIF = \left(\frac{\dot{\varepsilon}}{\dot{\varepsilon}_s}\right)^{1.026\alpha} \quad \text{for } \dot{\varepsilon} \le 30 s^{-1} \quad (1)$$

$$DIF = \gamma \left(\frac{\dot{\varepsilon}}{\dot{\varepsilon}_s}\right)^{1/3} \quad \text{for } \dot{\varepsilon} > 30 s^{-1} \quad (2)$$

Where:

$\dot{\varepsilon}$: **Strain rate**

$\dot{\varepsilon}_s = 30 \times 10^{-6}\ s^{-1}$ **(quasi-static strain rate)**

$\log\gamma = 6.156\alpha - 2$

$\alpha = 1/(5 + 9\frac{f'_c}{f_{co}})$

$f_{co} = 10MPa = 140psi$

In the numerical simulations the behavior of concrete was incorporated using damage plasticity model accessible within the code. In the Present study compression behavior of concrete was incorporated using the stress-strain curve proposed by Kent D.C and Park R. (1971). The tension behavior of concrete was predicted using Hillerborg's (1976) fracture energy criterion. The brittle fracture concept was used by Hillerborg to define the material parameter of Gf which is the needed energy to open a unit area of crack. With this approach stress displacement response determines the brittle behavior of concrete.

The approach of Sadique et al (2013) was used to calculate the fracture energy at high strain rate. So the displacement was enhanced two times and the dynamic tensile strength four times approximately. As Gf is the multiplication of displacement and strength, it was enhanced by 8 times. The material parameters for concrete are given in Table1.

Iqbal et al. (2012) studied the influence of strain rate by incorporating individual stress-strain curves of concrete at different strain rate. It was found that deformation increased consistently with a decrease in strain rate and the model without strain rate predicted higher deformation. In this study, however the constant strain rate of 100 s^{-1} was assumed. So the value of DIF was obtained to equal 2.32 from equation (2).

6. Dynamic Properties of Steel Reinforcement under High Strain Rates

The isotropic properties of metallic materials make it possible to assess the inelastic and elastic behavior to dynamic loading. Norris et al. (1959) tested two steel types with different static tensile yield strength of 330 and 278 MPa at strain rates varying between 10^{-5} and 0.1 s^{-1}. For the two steel types strength increase of 9 - 21% and 10 - 23 % were observed respectively. Dowling and Harding (1967) carried out tensile experiments on mild steel at strain rates varying between 10^{-3} s^{-1} and 2000 s^{-1}. It was concluded that mild steel is highly sensitive to strain rate. It was also found that mild steel with lower yield strength can almost be doubled; the upper yield strength can be considerably higher. On the other hand, the ultimate tensile strength can be increased by about 50%.The ultimate tensile strain increases with decreasing strain rate. Malvar (1998) studied the effect of high strain rates on the strength enhancement of steel reinforcing bars. DIF was proposed for for yield stresses, fy, between 290 and 710 MPa as represented by equation (3).

$$DIF = \left(\frac{\dot{\varepsilon}}{10^{-4}}\right)^{\alpha} \quad (3)$$

Where for calculating yield stress $\alpha = \alpha_{f_y}$,

$$\alpha_{f_y} = 0.074 - 0.04\left(\frac{f_y}{414}\right)$$

For ultimate stress calculation $\alpha = \alpha_{f_u}$,

$$\alpha_{f_u} = 0.019 - 0.009\left(\frac{f_y}{414}\right)$$

The material behavior of steel reinforcement was incorporated elasto-plastic material model in which compressive and tensile yield stresses were assumed equal to the steel yield stress. In the inelastic range of deformation the strain hardening of 2% was assumed. At 100 s^{-1} strain rate, DIF was obtained to equal 1.44 And 1.12 for yield and ultimate stress respectively. (Equation (3)). Table 2 shows

the material parameters for steel reinforcements.

7. RESULTS AND DISCUSSION

The local as well as global deformations of containment in concrete was measured and concrete damage parameters including tension and compression damage were evaluated at each impact location against each aircraft crash. The obtained results compared with those of the studies accessible in literature. It was found that the mid height of containment and center of the cylindrical portion experienced the highest deformation. In contrast to results obtained by Abbas et al. (1995, 1996), it became apparent that junction of cylindrical and dome is not most critical location.

The impact locations i.e., near the junction of dome and cylinder, mid height of containment,the center of cylindrical portion, and over the cylindrical portion close to the foundation were defined as location “D” , “C” , “B” and “A” respectively.

The peak displacement contours in the concrete at each impact location was represented in Fig. 4against the strike of 707-320. At locations “A” and “B” RCCV experienced the maximum displacement of 15.59 mm and 45.09 mm. At location “A”, it seems there is no study accessible in the literature against aircraft crash. Iqbal et al. (2012) worked on the behavior of BWR Mark III type nuclear containment subjected to Boeing 707-320 at the center of the cylindrical portion and reported the maximum deformation of 88.9 mm. However, no other result is accessible in literature to compare this observation. The peak deformation of concrete at the location “C” was found to be 45.86 mm.

The Controversial location in the literature is the linkage of cylinder and dome of containment building. At this location, Abbas et al. (1996), Kukreja (2005) and Iqbal et al. (2014) investigated the BWR Mark III type nuclear containment subjected to 707-320 and reported the maximum deformation of 34.2 mm, 46 mm and 66.98 mm respectively.

In this study, the maximum magnitude of deformation was noticed to be 35.37 mm at the same location. It can therefore be concluded that the center of cylindrical portion and mid height of containment experienced the highest deformation against normal strike of 707-320. Moreover, location “A” which was four meter above the foundation level, experienced the lowest displacement. The maximum deformation contour in concrete due to crash of A320 has been represented in Fig. 5. The highest

value of deformation in concrete is 13.64 mm and 36.07 mm at locations“A” and “B” respectively. At these locations against A320, it seems there is no results available in the literature to be compared. Iqbal et al. (2014) investigated BWR Mark III type nuclear containment subjected to the same aircraft and reported the maximum deformation of 74.52 mm at mid height of containment while 36.34 mm at junction of dome and cylinder.

Siefert and Henkel (2014) noticed a maximum displacement of 50 mm in an assumed containment building subjected to crash of A320 at the junction of dome and cylinder. It was observed that RCCV experienced the maximum displacement of 36.55 mm and 28.38mm at the locations “C” and “D” respectively. The peak magnitude of the deformation due to crash of A320 has been found to be lesser in comparison with 707-320 at each impact location.

Furthermore, it was noticed that the intensity of deformations were nearly equal at locations “B” and “C” subjected to A320. The peak intensity of deformation due to strike of F4 has been found to be 81.06 mm at impact location “B” while 38.44 mm at location “A” (Fig. 6). Peak deformation enhanced to 85.31 mm at location “C”. At junction of dome and cylinder, Frano and Forasassi (2011) observed a peak displacement of 217 mm in an IRIS containment while Abbas et al. (1996) noticed the peak deformation of 44.2 mm in a BWR containment against F4. However, in this study a maximum displacement of 67.07 mm has been noticed.

It was concluded that the maximum deformation of containment depends on the stiffness of strike location. Since mid height of the containment and center of cylinder portion are located in the cylindrical region which doesn’t have any influence of boundary conditions, experienced the highest deformation against all aircrafts crash. It can be found that location “A” is the most vigorous region, see Figs. 4–6.Displacement has decreased at location “D” due to the fact that structural stiffness in this region is higher as compared to strike locations “C” and “B”. Moreover, the maximum value of the deformation due to the crash of F4 has been found to be highest as compared to other two aircrafts at each impact location.

Table 3 indicates time at which deformation of containment reached its maximum value for each aircraft crash at impact locations.

Figs. 7-9 show the global deformation of containment measured along the

longitudinal orientation at different time intervals against F4, Boeing 707-320 and A320 respectively. The negative sign on horizontal axis shows below while positive sign above the center of impact. On vertical axis however, the positive sign indicates the outward while the negative sign inward deformation of the containment.

The deformation of the containment increased with increasing the magnitude of loading. The maximum deformation of the containment was noticed to be confined to the contact zone. Besides, during the loading time histories the global deformation of containment decreased as the loading started decreasing. Against strike of F4 at impact location "C", the profile of displacement was found to be almost symmetric about the impact location in the above and below the center of impact region at different time intervals, Fig. 7(c).

Against F4, rebounding of the structure was observed at location "A" on the descending branch of loading at time interval 0.064 s and 0.075 s, please see Fig. 7(a). Furthermore, outward deformation did not observe at none of impact location against crash of F4 (Fig. 7).

Against strike of 707-320, outward deformation was noticed away from impact region at time interval 0.3 s at location "A" and "B" (Fig. 8 (a) and (b)). Outward displacement even observed in impact zone at impact locations "D" and "C" when the loading was decreasing to zero, please see the profile at time interval 0.3 s in Fig. 8(c) and (d). Outward displacement of RCCV was also observed against crash of A320 at each impact locations at time interval 0.232 s and 0.25 s, see Fig. 9. In general, outward deformation of containment along longitudinal orientation occurred on the descending branch of loading time histories and no sign of outward deformation was observed before maximum loading.

Figs. 10–13 show the tension damage occurred in the concrete against strike of aircrafts for different strike locations of "A", "B", "C", and "D" respectively. Figures comprise three pairs of contours (designated as (A), (B) and (C)), indicating tension damage due to strike of A320, 707-320 and F4 respectively. (a1), (b1) and (c1) highlights parameter of tension damage, dt, at the outer face of the containment, while (a2), (b2) and (c2) indicates dt at the inner face of the containment. The compression and tension damage in concrete has been assumed to occur when the damage parameters, dt and dc, has exceeded the value of 0.9. Against A320, no sign of tension damage was observed at both the

inner and outer face of containment at impact location "A" and "D" (Fig. 10(A) and 13(A)). Inside of RCCV experienced some local tension damage against crash of 707-320 and F4 at impact locations "A" and "D". However, it was not remarkable and spread over a small area, see Figs. 10(b2) and (c2) and 13(b2) and (c2). A more extensive region found to be damaged due to crash of F4 as compared to 707-320. Tension damage in concrete was also observed around the strike region at the outer face of RCCV due to strike of F4 at location "D" (Fig. 13(c1)). At impact locations "B" and "C" a major region has been observed to be damaged at the inner face of RCCV as compared to locations "D" and "A" . Moreover, a more extensive region at impact location "B" damaged in tension as compared to location "C", please see Figs. 11 and 12.

Furthermore, at the outside of RCCV a wider region found to be damaged at impact location "B" due to strike of F4 as compared to 707-320 (Fig.11 (c1) and (b1)). Against A320, at impact location "C" and "B" tension damage wasn't noticed at the outer face of containment (Figs. 11(a1) and 12(a1)). Due to crash of all aircrafts at location "A" and strike of 707-320 and F4 at location "B", tension damage has also been observed at the outer face of containment close to the foundation; see Fig. 10 and Fig. 11(b1) and (c1). Furthermore, lesser damage was observed at the linkage of dome and cylinder as compared to midpoint of cylindrical portion and mid height of containment.

The concrete damage in tension has been also found to occur around the impact region at the outer face of the containment (Fig. 11(b1) and (c1), Fig. 12(c1) and Fig. 13(c1)). Moreover, Tension damage was not observed at the dome of RCCV due to aircrafts crash at impact locations. Generally, local failure of containment was noticed around the impact location and global failure of containment did not occur due to strike of aircrafts crash at impact locations. It may be concluded RCCV is able to withstand the strike of A320, Boeing 707-320 and Phantom F4.

At each impact location, two elements which experienced maximum compression damage has been chosen at the outer face of containment (Fig. 3). The variation of compression damage with respect to time has been represented for selected elements of concrete in Fig. 14.

It was observed compression damage for elements at the outer face of containment could not reach the damage threshold at

none of impact locations for any aircraft crash. So it may be concluded that d_c is not critical and $d_t$is prominent. It has been also found that at each impact location the significant tension damage of concrete occurred at the inner face the strike region. while no sign of tension damage could be seen in the impact region at the outer face and this region is dominantly under compression. So it may be deduced that application of impact load has caused punching failure mechanism to the containment.

Global deformation of containment along circumferential orientation was also studied. The profiles of maximum deformation at impact locations was compared in Fig. 15. It can be seen the magnitude of the maximum deformation at location "A" due to strike of aircrafts was the smallest, while location "B" and "C" experienced the highest displacement. Along circumferential orientation, profile of displacement were in agreement for impact locations except location "A" at which deformation decreased to zero beyond 8 m away from center of impact region. Moreover, both inward and outward displacements were observed along circumferential orientation, see Fig. 15.

It is important to mention here that obtained results are solely based on the material behavior of concrete which is affected by strain rate and DIF as defined in sections 4-5. However, in the present study the constant strain rate of 100 s^{-1} has been considered in all of the models. This assumption made it possible to compare destructive power of aircrafts crash and vulnerability of impact locations.

Table 1: Material properties for concrete

Compressive strength (Mpa)	**30**
Density (kg/m^3)	**2400**
Dilation angle	**30**
Eccentricity	**1**
Initial equi-biaxial compressive yield stress to initial uniaxial Compressive yield stress, fb0/fc0	**1.16**
Bulk modulus, K	**0.666**
Modulus of elasticity, E(N/m2)	**2.7386E10**
Poisson's ratio, ϑ	**0.17**

Table 2: Material properties for steel reinforcement

Yield stress (N/mm^2)	**490**
Young's modulus; E(N/mm^2)	**2×10^5**
Density (kg/m^3)	**7850**
Poisson's ratio, ϑ	**0.33**
Strain hardening (in the inelastic range of deformation)	**2%**

Table 3: Time of maximum deformation at impact locations against each aircraft crash

	Location "A"	Location "B"	Location "C"	Location "D"
Phantom F4	**0.046 s**	**0.054 s**	**0.053 s**	**0.051 s**
Boeing 707-320	**0.208 s**	**0.235 s**	**0.233 s**	**0.232 s**
Airbus A320	**0.133 s**	**0.165 s**	**0.162 s**	**0.157 s**

s: second

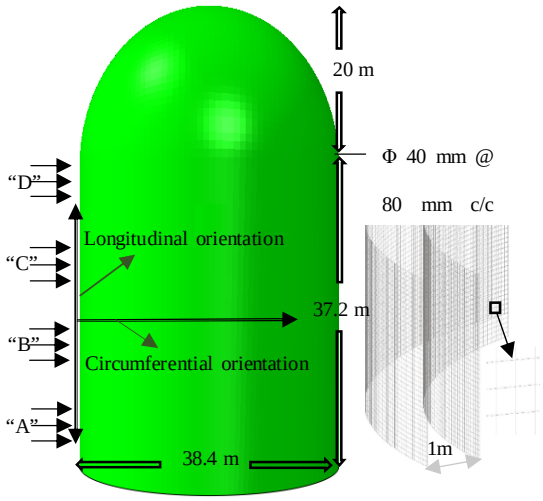

Fig. 1. Geometric model of RCCV and selected impact locations

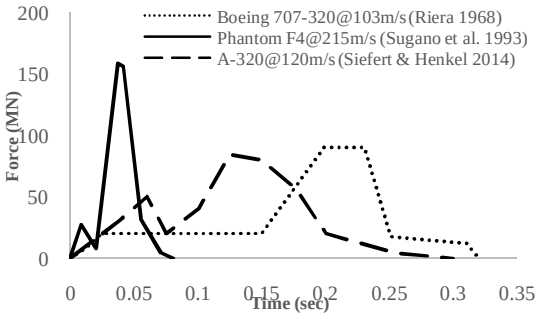

Fig. 2. Loading time history for aircrafts

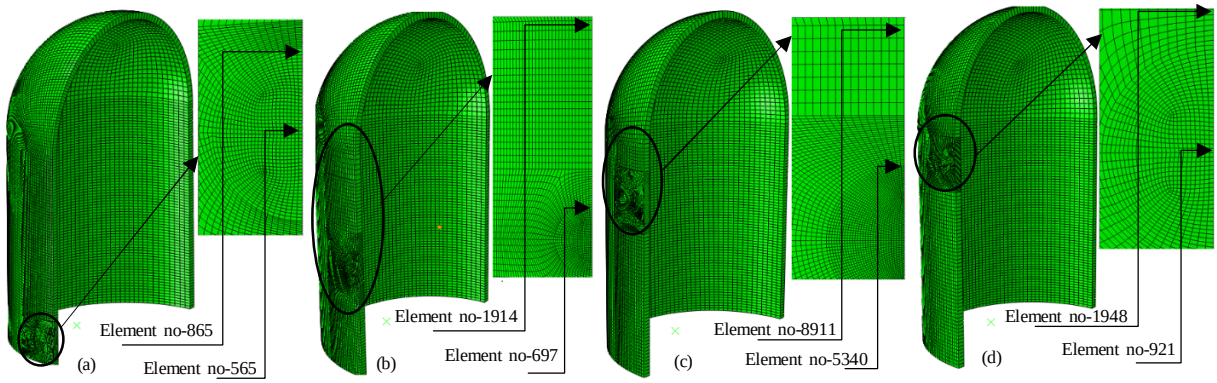

Fig. 3. Finite element model of the containment and selected elements at the outer face of the containment to plot compression damage at: (a) location "A", (b) location "B", (c) location "C" and (d) location "D".

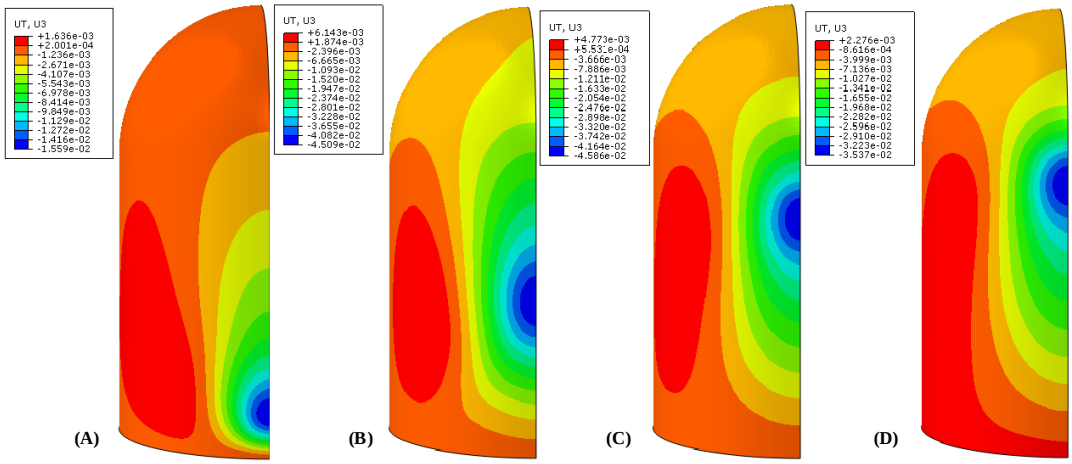

Fig. 4. Maximum displacement (in meter) in concrete in the direction of loading due to impact of 707-320 at: (A) location "A" , (B) location "B" , (C) location "C" and (D) location "D".

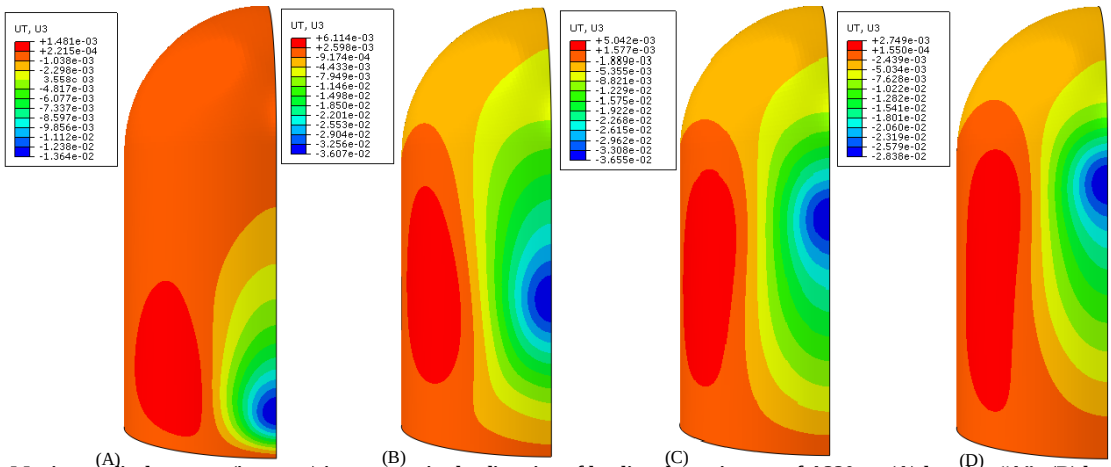

Fig. 5. Maximum displacement (in meter) in concrete in the direction of loading due to impact of A320 at: (A) location "A" , (B) location "B" , (C) location "C" and (D) location "D".

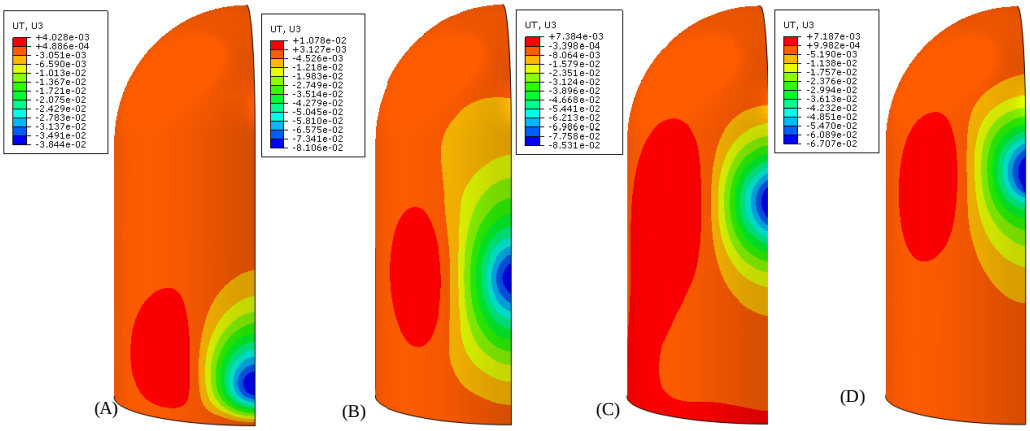

Fig. 6. Maximum displacement (in meter) in concrete in the direction of loading due to impact of Phantom F4 at: (A) location "A" , (B) location "B" , (C) location "C" and (D) location "D".

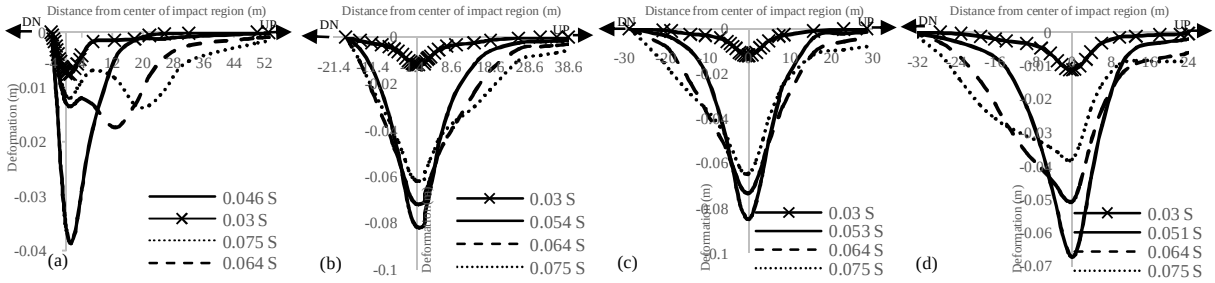

Fig. 7. Global deformation of the RCCV along the longitudinal orientation subjected to F4 at: (a) location "A", (b) location "B", (c) location "C" and (d) location "D" at different time intervals.

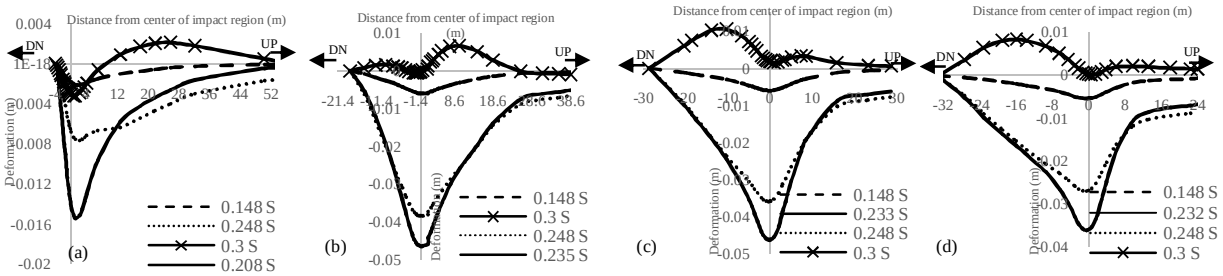

Fig. 8. Global deformation of the RCCV along the longitudinal orientation subjected to 707-320 at: (a) location "A", (b) location "B", (c) location "C" and (d) location "D" at different time intervals.

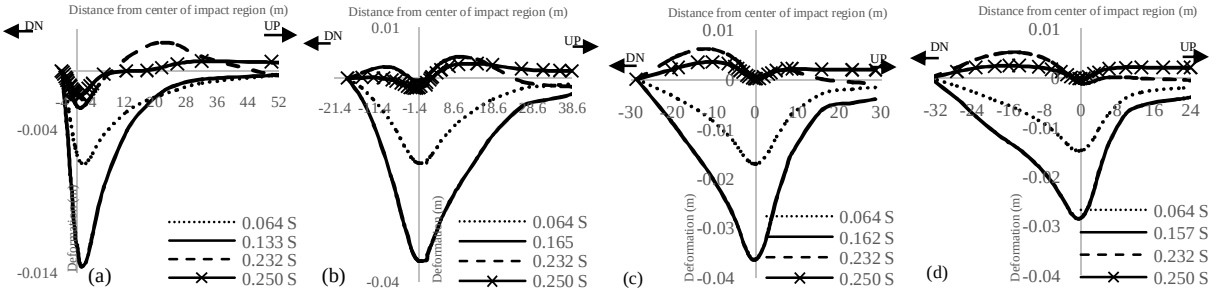

Fig. 9. Global deformation of the RCCV along the longitudinal orientation subjected to A320 at: (a) location "A", (b) location "B", (c) location "C" and (d) location "D" at different time intervals.

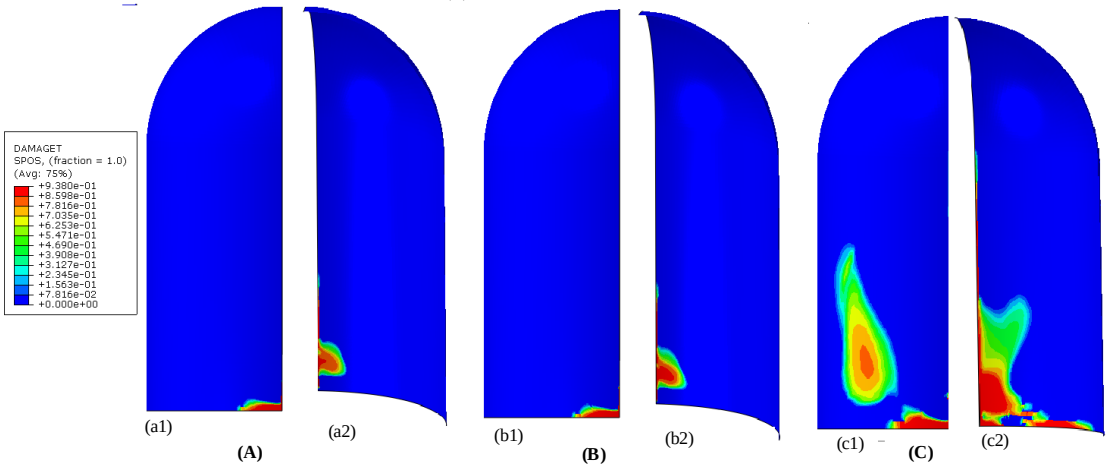

Fig. 10. Tension damage contours of concrete at the inner and outer face of containment at location "A" against: (A) Airbus A320, (B) Boeing 707-320 and (C) Phantom F4.

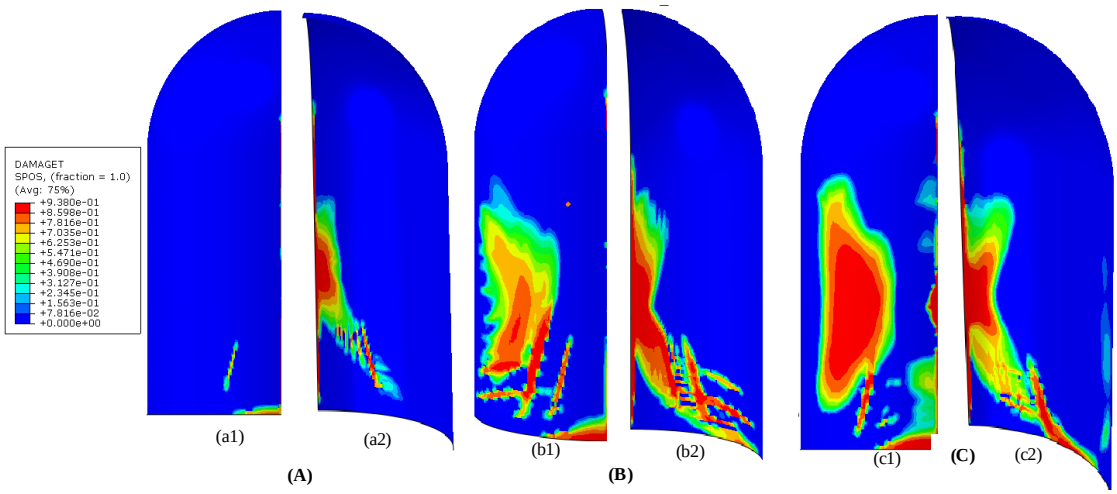

Fig. 11. Tension damage contours of concrete at the inner and outer face of containment at location "B" against: (A) Airbus A320, (A) Boeing 707-320 and (C) Phantom F4.

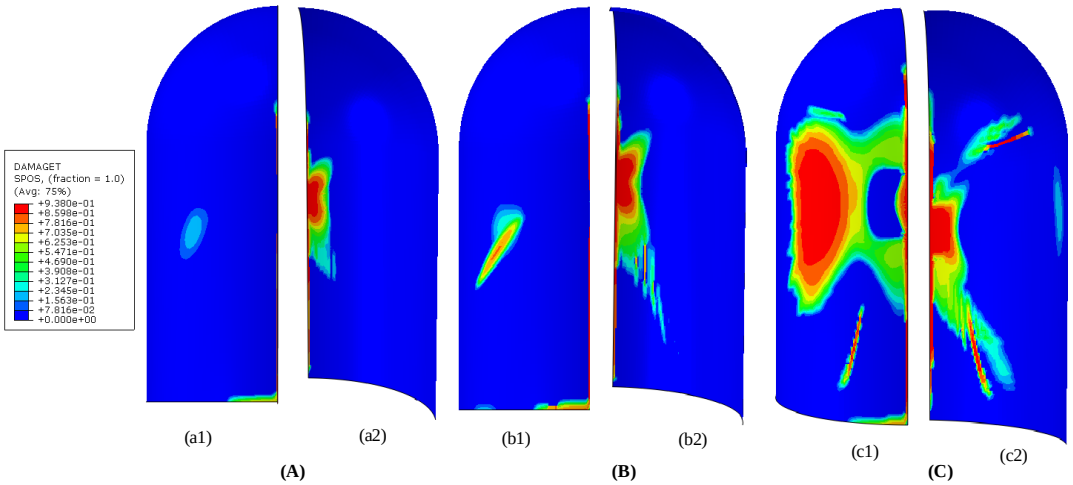

Fig. 12. Tension damage contours of concrete at the inner and outer face of containment at location "C" against: (A) Airbus A320, (B) Boeing 707-320 and (C) Phantom F4.

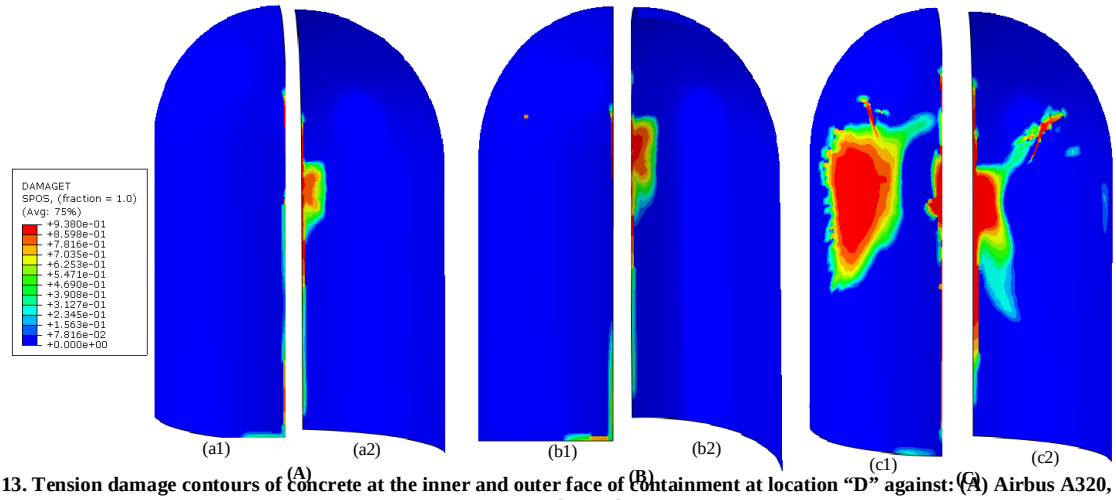

Fig. 13. Tension damage contours of concrete at the inner and outer face of containment at location "D" against: (A) Airbus A320, (B) Boeing 707-320 and (C) Phantom F4.

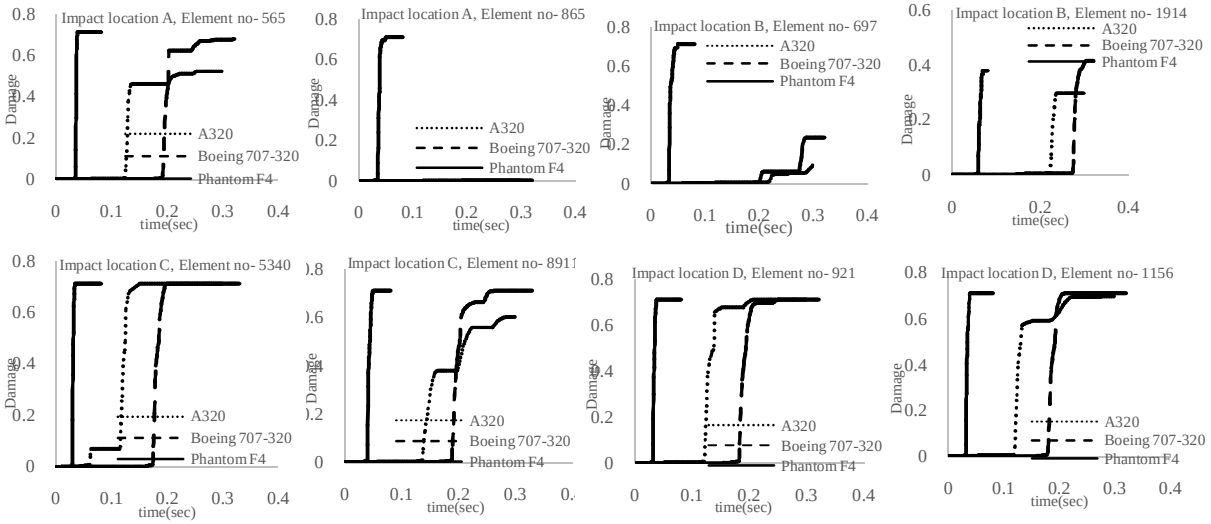

Fig. 14. Compression damage in concrete at different locations against aircraft crash

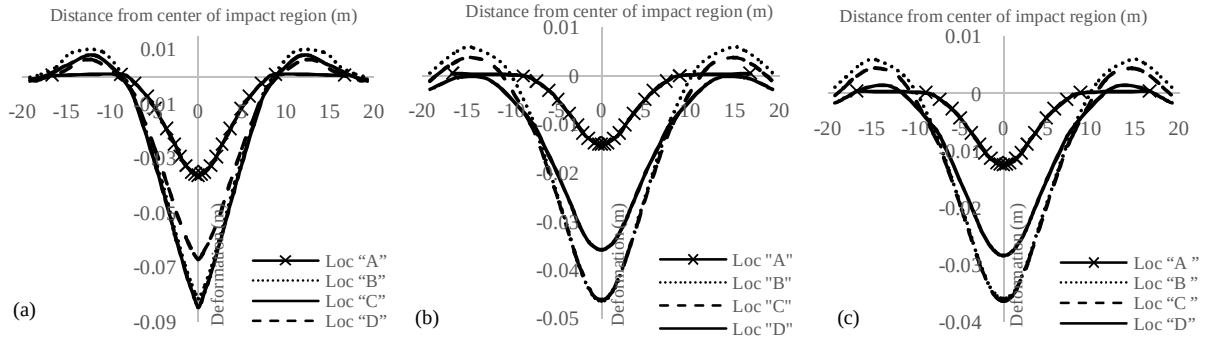

Fig. 15. Maximum deformation of the containment along the central circumferential orientation at impact locations against: (a) F4, (b) Boeing 707-320, (c) A320.

CONCLUSION

Response of nuclear containment was studied against strike of Boeing 707-320, Phantom F4and Airbus A320 aircrafts at four different impact locations:

Location “A”: 4 m above the foundation level

Location “B”: center of cylindrical portion

Location “C”: mid height of containment

Location “D”: near the junction of cylinder and dome

The highest displacement at impact locations was observed due to strike of F4.

Moreover, the severity of displacement (in direction of loading) at impact location “C” and “B”has been noticed to be maximumdue to aircrafts crash.

The deformation along the longitudinal orientation was observed to be spread over a

larger area as compared to that of along the circumferential orientation of the containment. It was in agreement with that of results available in literature. Phantom F4 also caused severe damage as compared to other two aircrafts. While A320 behaved like a crushable missile and caused so negligible damage at each impact location.

It was also found that compression damage is not prominent and damage of concrete is critical under tension. The center of cylinder portion was found to be the most critical impact location at which RCCV experienced the largest damaged area. However, it was concluded that RCCV was able to sustain the direct strike of aircrafts and global failure of containment did not occur against any aircraft.

REFERENCES

[1] Abaqus Explicit user manuals Version 6.12.

[2] Abbas, H., Paul, D. K., Godbole, P. N., & Nayak, G. C. (1995). "Reaction-time response of aircraft crash". Computers & structures, Vol. 55, No. 5, pp. 809-817, DOI: 10.1016/0045-7949(94)E0270-C.

[3] Abbas, H., Paul, D. K., Godbole, P. N., & Nayak, G. C. (1996). "Aircraft crash upon outer containment of nuclear power plant". Nuclear Engineering and Design, Vol. 160, No. 1, pp. 13-50, DOI: 10.1016/0029-5493(95)01049-1.

[4] Arros, J., & Doumbalski, N. (2007). "Analysis of aircraft impact to concrete structures". Nuclear engineering and design, Vol. 237, No. 12, pp. 1241-1249, DOI:10.1016/j.nucengdes.2006.09.044.

[5] CEB-FIP Model code (2010), International Federation for Structural Concrete.

[6] Chelapati, C. V., Kennedy, R. P., & Wall, I. B. (1972). "Probabilistic assessment of aircraft hazard for nuclear power plants". Nuclear Engineering and Design, Vol.19, No. 2, pp. 333-364, DOI: 10.1016/0029-5493(72)90136-7.

[7] Dowling, A.R. and Harding, J. (1967), "Tensile properties of mild steel under high strain rates", Proceedings of the 1st HERF Conf., University of Denver, Colorado.

[8] Eric W. Klamerus and J. Davis (2002), "Structural seismic fragility analysis of the surry containment", U.S. Nuclear Regulatory Commission, Washington, DC 20555-0001, NRC Job Code W6487.

[9] Hillerborg, A., Modéer, M., & Petersson, P. E. (1976). "Analysis of crack formation and crack growth in concrete by means of fracture mechanics and finite elements". Cement and concrete research, Vol. 6, No. 6, pp.773-781, DOI: 10.1016/0008-8846(76)90007-7.

[10] Iliev, V., Georgiev, K., & Serbezov, V. (2011). "Assessment of impact load curve of Boeing 747-400". MTM Virtual, Vol. 1, pp.22-25.

[11] Iqbal, M. A., Rai, S., Sadique, M. R., & Bhargava, P. (2012). "Numerical simulation of aircraft crash on nuclear containment structure". Nuclear Engineering and Design, Vol. 243, pp. 321-335, DOI: 10.1016/j.nucengdes.2011.11.019

[12] Iqbal, M. A., Sadique, M. R., Bhargava, P., & Bhandari, N. M. (2014). "Damage assessment of nuclear containment against aircraft crash". Nuclear Engineering and Design, Vol. 278, pp. 586-600, DOI: 10.1016/j.nucengdes.2014.07.040.

[13] Jiang, H., & Chorzepa, M. G. (2014). "Aircraft impact analysis of nuclear safety-related concrete structures: A review". Engineering Failure Analysis, Vol. 46, pp. 118-133. DOI: 10.1016/j.engfailanal.2014.08.008.

[14] Kent D.C and Park R. (1971), "Flexural Members with Confined Concrete". Journal of Structural Division, Vol 97, No. 7, pp.1969-1990.

[15] Lo Frano, R.L., Forasassi, G., (2011). "Preliminary evaluation of aircraft impact on a near term nuclear power plant". Nuclear Engineering and Design, Vol. 241, No.12, pp. 5245–5250. DOI:10.1016/j.nucengdes.2011.08.079.

[16] Lu, Y., & Xu, K. (2004). "Modelling of dynamic behavior of concrete materials under blast loading". International Journal of Solids and Structures, Vol. 41, No. 1,pp.131-143, DOI:10.1016/j.ijsolstr.2003.09.019.

[17] Malvar, L. J., (1998). "Review of static and dynamic properties of steel reinforcing bars". ACI Materials Journal-American Concrete Institute, Vol. 95, No. 5, pp. 609-616.

[18] Ngo, T., Mendis, P., Gupta, A., & Ramsay, J. (2007). "Blast loading and blast effects on structures–an

overview". Electronic Journal of Structural Engineering, Vol. 7, pp. 76-91.

[19] Ngo, T., Mendis, P., Hongwei, M., & Mak, S. (2004). "High strain rate behavior of concrete cylinders subjected to uniaxial compressive impact loading". In Proc. of 18th Australasian Conference on the Mechanics of Structures and Materials.

[20] Norris, G.H., Hansen, R.J., Holly, M.J., Biggs, J.M., Namyet, S. and Minami, J.K. (1959). "Structural design for dynamic loads", McGraw-Hill, New York, USA.

[21] Riera, J. D. (1968). "On the stress analysis of structures subjected to aircraft impact forces". Nuclear Engineering and Design, Vol. 8, No. 4, pp. 415-426, DOI: 10.1016/0029-5493(68)90039-3.

[22] Riera, J. D. (1980). "A critical reappraisal of nuclear power plant safety against accidental aircraft impact". Nuclear Engineering and Design, Vol. 57, No. 1, pp. 193-206, DOI: 10.1016/0029-5493(80)90233-2.

[23] Sadique, M. R., Iqbal, M. A., & Bhargava, P. (2013). "Nuclear containment structure subjected to commercial and fighter aircraft crash". Nuclear Engineering and Design, Vol. 260, pp.30-46, DOI: 10.1016/j.nucengdes.2013.03.009.

[24] Siefert, A., Henkel, F.O., (2014). "Nonlinear analysis of commercial aircraft impact on a reactor building - comparison between integral and decoupled crash simulation". Nuclear Engineering and Design, Vol. 269, pp. 130-135, DOI:10.1016/j.nucengdes.2013.08.018.

[25] Sugano, T., Tsubota, H., Kasai, Y., Koshika, N., Orui, S., Riesemann, W.A.V., Bickel, D.C.,Parks, M.B., 1993. "Full-scale aircraft impact test for evaluation of impact force". Nuclear Engineering and Design, Vol. 140, pp. 373–385.